



## The Influence of Heat Treatment on Tribological Properties of Cu-Al-Fe-Ni Shape Memory Alloy

M.M. Sadawy\*

*Mining and Pet. Dept, Faculty of Engineering, Al-Azhar University, Nasr City, Cairo, Egypt.*

### ARTICLE INFO

#### Article history:

Received 06 October 2019  
Received in revised form  
18 December 2019  
Accepted 10 January 2020  
Available online 15 January  
2020

#### Keywords:

1<sup>st</sup> Copper alloys  
2<sup>nd</sup> Shape memory alloys  
3<sup>rd</sup> Aging  
4<sup>th</sup> Wear resistance  
5<sup>th</sup> Worn morphology

### ABSTRACT

The effect of heat treatment on tribological properties of Cu-Al-Fe-Ni alloy under dry conditions was investigated. Scanning electron microscopy (SEM) associated with energy-dispersive X-ray spectroscopy (EDX) was used to evaluate the microstructure. Dry sliding wear tests were conducted on the as-cast and heat treated samples using pin on disc machine at different applied loads (10,15,20,25 and 30 N) and sliding speed ( 1.0 , 2.0,3.0 ,4.0 and 5.0 m/s). The results showed that aging the alloy at 350 °C resulted in formation of fine alpha grains and fine  $\kappa$ -phase compared with the cast condition. These fine phases could improve the wear resistance of the investigated alloy. However, the hardness and the wear resistance decreased when the aged temperature increased. Furthermore, the results indicated that the average contact surface temperature in the wear test increased with increment of aging temperature. On the other hand, the worn surfaces revealed that the predominant wear mechanism was abrasive wear.

### 1. Introductions

Copper-based alloys have been extensively used in many industrial applications, such as aerospace, automobile, marine and machinery owing to their thermal conductivity, good electrical conductivity, excellent ductility and corrosion resistance [1–4]. Furthermore, the copper-based alloys have ability to exhibit the shape memory effect within a certain range of compositions which have a disordered body center cubic structure (bcc), called  $\beta$ -phase, which is stable at high temperature [5]. Shape memory alloys (SMAs) belong to a group of functional, smart materials with the unique property of “remembering” the shape they had before pseudo plastic deformation. Such an effect is based on crystallographic reversible thermo-elastic martensitic transformation [6]. Cu-based SMAs, especially Cu–Al–Ni and Cu–Al–Mn, are commercially available and they have some advantages over Ni–Ti and other shape memory alloys such as low melting point , composition control, good castability, better

machinability and higher Young’s modulus [7,8]. Aluminum as the major alloying element would result in higher strength and enhancement in the corrosion resistance by formation of an oxide/hydroxide film. Cu–Al–Ni alloy do not contain any solid lubricant like lead in leaded bronzes. Therefore, their wear behaviour should be different than that of leaded bronzes in identical operating conditions [9]. Cu–Al–Ni can be heat treated to produce different structures with many phases. Recently, considerable research has been carried out to characterize microstructure, mechanical properties and corrosion behaviors of as-cast Cu–Al alloy [10]. It was reported that the precipitation of  $\kappa$ -phases with different chemical composition from different heat treatment conditions led to the changes of mechanical behaviours of Cu–Al alloy [11]. Chen et al. [12] found that heat treatment, in the sequence of quenching, normalizing and aging, improved the tensile strength but at the expense of ductility. Furthermore, the shape memory properties of Cu–Al – Ni can be modified by several factors. The heat treat-

\*E-mail address: [mosaadsadawy@yahoo.com](mailto:mosaadsadawy@yahoo.com).

ment is one of them that can control the shape and size of these precipitates [8]. However, the data available on their wear behaviour is low.

In the present study, an attempt has been made to investigate the effect of heat treatment on the tribological properties of Cu-Al-Fe-Ni alloy under dry conditions. The effects of normal load and sliding velocity on wear performance were investigated. The morphology and composition of the worn surface were also analysed. The corresponding mechanism was also discussed.

## 2. Materials and methods

### 2.1. Materials

The investigated alloy was fabricated from high purity Cu, Al, Fe and Ni. A measured weight of Cu was melted in a muffle furnace to a temperature of 1200°C. After melting appropriate amounts of Al, Fe and Ni were added gradually and respectively under nitrogen gas. The melt was mechanically stirred for 5 min. A Schematic diagram during melt stirring is shown in Fig.1. The melt was casted into stainless steel mold of dimensions (200×50×20 mm) and naturally cooled down to room temperature. The chemical composition of the alloy as shown in Table 1 was determined by X-ray fluorescence (XRF). The alloy was cut into samples with dimensions of 50×10×10 mm.

Table1. Chemical Composition (wt %) of the Investigated Alloy

Element	Al	Fe	Ni	Pb	Sn	Cr	Cu
Wt.%	11.13	2.32	1.71	0.016	0.02	0.001	Bal.

### 2.2. Heat-treatment

The heat treatment of the investigated alloy was performed in electric muffle furnace. The temperature was regulated using a temperature regulator of accuracy  $\pm 1.0^\circ\text{C}$  coupled with thermocouple (K-Type) to obtain the actual sample temperature. The as-cast samples were first heat treated at 960 °C for 5 hours to dissolve all phases and transform the entire matrix into martensite phase. Then they removed and directly quenched in the water for 5 minutes. After that these samples were aged at different temperatures (350, 450, 550 and 650 °C respectively) for 5 hours and cooled in water.

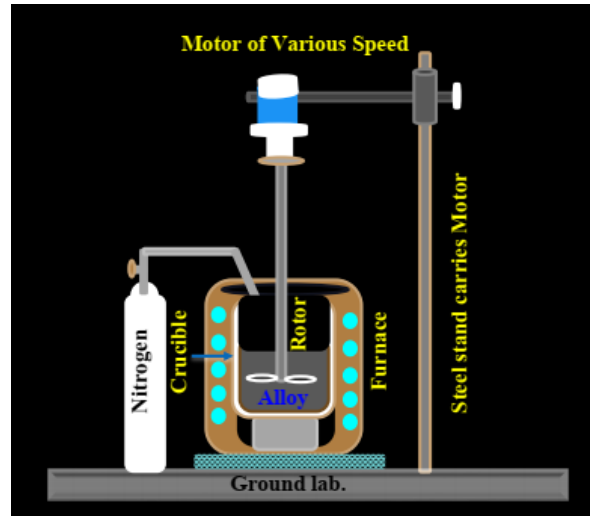


Fig.1. A Schematic diagram for melt stirring process

### 2.3. Microstructure evolution

The microstructure of as-cast and heat treated samples were analyzed using scanning electron microscopy (SEM) with energy-dispersive X-ray spectroscopy (EDX) (model JEOL JSM-6330F at a voltage of 20 keV). All samples were prepared by grinding with 500, 600 800, 1000 and 1200 grit SiC paper respectively. After that, these samples were polished using 6, 3 and 1  $\mu\text{m}$  diamond paste. The surfaces of samples were cleaned using acetone and dried in air. The samples were etched in solution composed of 5g  $\text{FeCl}_3 + 25 \text{ mL HCl} + 50 \text{ mL H}_2\text{O}$ .

### 2.4. Hardness

The hardness of the as-cast and heat treated samples was measured in a Vickers hardness tester using a load of 5 kg. In each sample, 10 indentations were taken and the average hardness value was taken.

### 2.5. Sliding wear test

The wear behaviour of the as-cast and heat treated samples was evaluated using pin-on-disc machine. The applied loads were 10, 15, 20, 25 and 30 N respectively. The sliding speeds were 1.0, 2.0, 3.0, 4.0 and 5.0 m/s at a constant time limit of 10 minutes. Fig. 2 shows the schematic diagram of pin-on-disc machine.

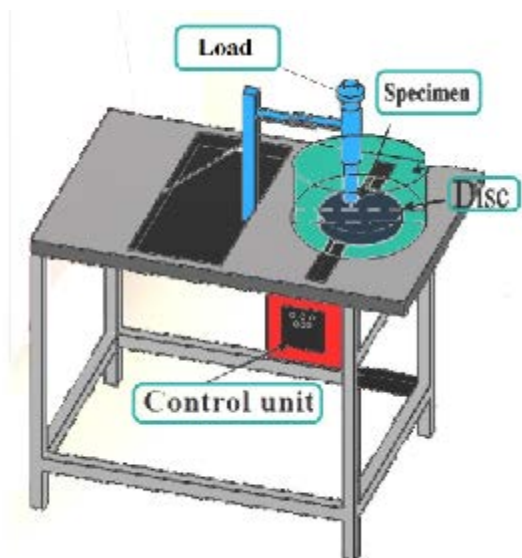


Fig.2. Schematic diagram of pin-on-disc test set up

The sliding was performed on 600 grit SiC paper fixed on an aluminium wheel on the pin-on-disc machine. During sliding, the load was applied on the specimen through a cantilever mechanism and the specimen brought in intimate contact with a rotating disc with a diameter of 140 mm.

The specimens were weighed with a digital balance with a sensitivity of  $10^{-4}$  g. The wear rates were obtained from the volume lost after sliding wear tests using Archard equation [9]:

$$V = \frac{KW}{H} \quad (1)$$

where V is the volume loss of the abraded material per unit sliding distance, K is the wear coefficient, W is the applied normal load and H is the hardness of the abraded material.

After wear test the abraded material was collected and analyzed using XRD diffraction to determine the different phases of abraded material. A computer controlled X-ray (Philips Analytical X-ray B.V. Machine) with monochromatic Cu-K radiation was used.

The morphology of wear tests for all specimens was also investigated using optical microscope. Moreover, the surface roughness was evaluated using mountain software (MountainsMap® Premium 7.4) after wear tests.

## 2.6. Temperature measurement

Temperature measurements of wear pin during the sliding were carried out with thermocouple (K-Type). Thermocouples were placed into a hole of 2 mm diameter at 1.5 mm away from sliding surface drilled up at axis of cylindrical pin. Temperature was recorded with help of digital temperature indicator.

## 3. Results and Discussions

### 3.1 Microstructure evolution

The microstructure of as-cast and heat treated Cu-Al-Fe-Ni alloy is presented in Fig. 3. The structure as shown in Fig. 3(a) is characterized by coarse  $\alpha$ - phase and coarse martensite  $\beta$ -phase. The white regions in SEM micrographs represent primary  $\alpha$  structure, while the black regions on the grain boundaries are secondary phase ( $\beta$ ). The micrographs show that the  $\beta$ -phase distributes along the grain boundaries.

Fig.3 (b) reveals that water quenching of the alloy from the solutionization temperature of 960 °C to room temperature transformed all the  $\beta$  phase into  $\beta'$  phase structure which is a supersaturated solid solution. The volume fraction of  $\beta'$  increases due to the dissolution of  $\alpha$  and  $\kappa$  phases. Therefore, the microstructure of the alloy is significantly different from those of the as-cast, although the sample still consists of  $\alpha$ ,  $\alpha$ -phase and  $\beta$ -phase. Wu et al. [10] found that the volume fraction of the  $\beta$ - phase increases greatly, which is attributed to the transformation of the initial  $\alpha$  and  $\kappa$  phases into  $\beta$ -phase.

On the other hand, aging the solution heat treated sample at 350 and 450 °C as shown in Fig.3 (c&d) transforms certain amount of martensitic ( $\beta$ ) phase into fine  $\alpha$  grains and dispersed precipitates of  $\kappa$  and  $\gamma_2$  phases. Increasing the aging temperature to 550 °C and 650 °C transforms martensitic ( $\beta$ ) phase into dispersed precipitates of  $\alpha$  and  $\gamma_2$  phases with large amount of coarse  $\alpha$ - phase as shown in Fig.3(e &f). The results are in a good agreement with the literature values [9 - 11]. The EDX analysis as shown in Fig 4 reveals that the  $\alpha$ -phase and  $\beta$ -phase at spot sites are composed of Cu and Al.

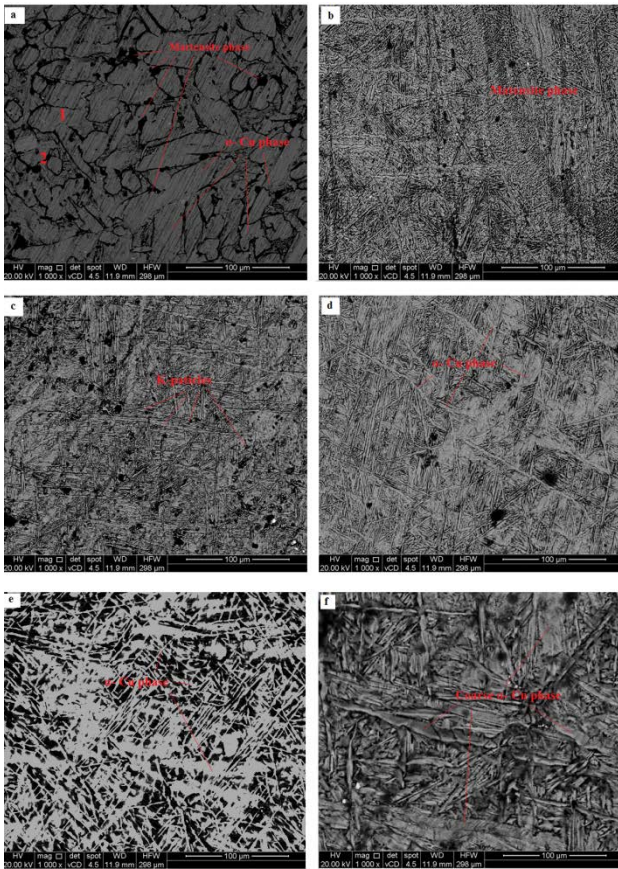


Fig.3. Microstructure of heat treated Cu-Al-Fe-Ni alloy. [(a) As-cast (b) Sol. heat treated, (c) 350 °C, (d) 450 °C, (e) 550 and (f) 650 °C

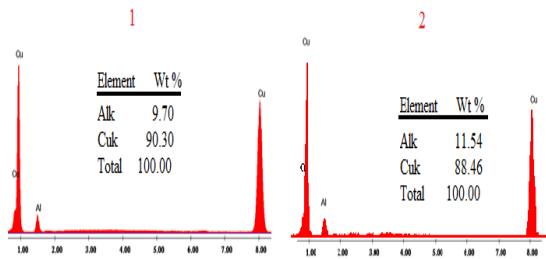


Fig.4. EDX results of as-cast Cu-Al-Fe-Ni at spotted points

### 3.2. Hardness measurements

Vickers hardness values of as-cast and heat treated Cu-Al-Fe-Ni alloy are shown in Fig. 5. It is obvious that increasing aging temperature, the hardness value decreases. It reaches its minimum peak at 650 °C. This behaviour is attributed to transforming martensitic

phase into dispersed precipitate of  $\alpha$  phase. It is known that  $\alpha$ -phase is softer than the  $\beta$  phase, so the hardness decreases. Moreover, Fig. 5 shows that the specimen aged at 350 °C has the highest hardness values when compared with the other samples. This behaviour is attributed to the k-phase precipitated during aging at 350 °C is finer than that precipitated during other aged conditions [6,8]. The hardness values are in agreement with the microstructural findings.

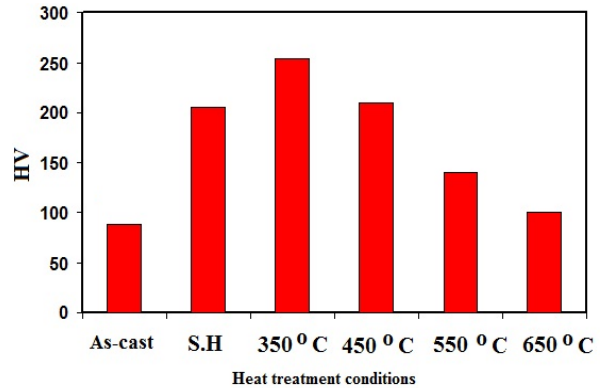


Fig. 5. Effect of heat treatment on hardness of Cu-Al-Fe-Ni alloy

### 3.3. Wear behaviour

#### 3.3.1. Effect of normal load

The wear rate of the as-cast and heat treated specimens as a function of applied load is shown in Fig. 6. It can be seen that increment of the normal load, an increase in wear rate is obtained for all specimens. The behaviour may be attributed to at lower load the contact area is less and hence reduces wear rate for the investigated samples while at higher loads, the contact area is more, causing an increase in wear rate [9]. Comparing the results of the investigated samples presented in Fig 6, it can be observed that the aged sample at 350 °C offers a superior wear resistance. Furthermore, the result in Fig. 6 shows that the wear rate increases with increasing aging temperature. Additionally, transition zones were observed for the as-cast and aged samples at 550 and 650 °C. These transition zones are established due to a sudden increase in the wear rate. However, these zones depend on the aged conditions. Clearly, the sample aged at 550 and 650 °C indicate transition zones from mild to severe wear at applied load of 25 N. The behaviour is attributed to transforming large amount of  $\beta$ -phase into

$\alpha$ -phase which is softer than  $\beta$ -particles for aged alloys. Further, the as-cast shows transition zone at a lower value (20 N) comparing to samples aged at 550 and 650 °C. This is due to as-cast alloy contains huge grains of  $\alpha$ -phase.

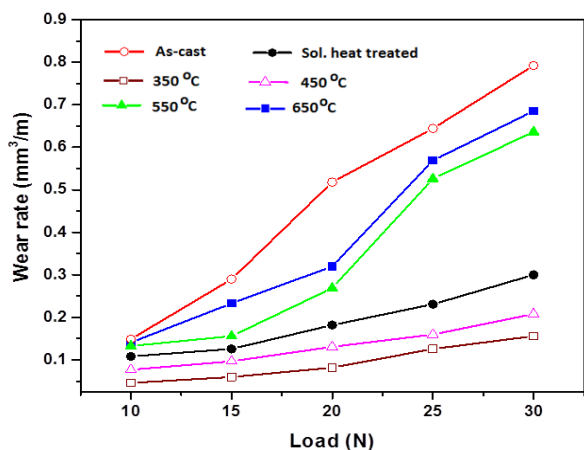


Fig.6. Effect of normal load on wear rate of the as-cast and heat treated Cu-Al-Fe-Ni alloy

### 3.3.2. Effect of sliding speed

The variation of wear rate with respect to sliding speed at a constant load of 15 N is shown in Fig. 7. It is obvious that increment of sliding speed from 1.0 to 5.0 m/s, the wear rate increases. However, the gradient of increasing in wear rate is not the same for the different heat treatment samples. It can be noted that the aged sample at 350 °C offers the lowest wear rate due to precipitating of fine k-particles. Also it can be seen that the wear rate increases with rising the aging temperature. This behaviour as discussed before is attributed to decreasing the  $\beta'$ -phase content. Moreover, Fig. 7 reveals that the as-cast and aged samples at 550 and 650 °C suffer from sudden increase in the wear rate at sliding speed of 4m/s. This is due to presence of coarse particles of k and  $\alpha$  which are softer than both fine k and  $\beta'$ -phase.

### 3.3.3. Morphology

Fig. 8 shows the micrographs of the worn surfaces of as-cast and heat treated Cu-Al-Fe-Ni alloy at load of 15N and sliding speed of 3.0 m/s. It is obvious that the worn surfaces of all samples are covered with continuous grooves and scratches parallel to the sliding direction. The grooves and scratches resulted from the ploughing action [13-19]. Moreover, Fig. 8 shows that

the predominant wear mechanisms are abrasion for all samples. However, the aged sample at 350 °C offers poorer wear behaviour and narrow grooves with lower depth on the worn surfaces. This behaviour is due to the k-phase precipitated during aging at 350 °C is finer than that precipitated during other aging conditions.

On the other hand, Fig. 8 shows that the width and depth of the grooves increase with the increase of ageing temperature due to transforming large amount of  $\beta$ -phase into precipitates of  $\alpha$ -particles which are softer than  $\beta$ - particles.

The XRD analysis was performed on the abraded powder for specimen aged 350 °C as shown in Fig 9. The results show that the powder composed of Cu, Cu<sub>4</sub>Al<sub>9</sub>,  $\beta$ - and Fe<sub>3</sub>Al phases.

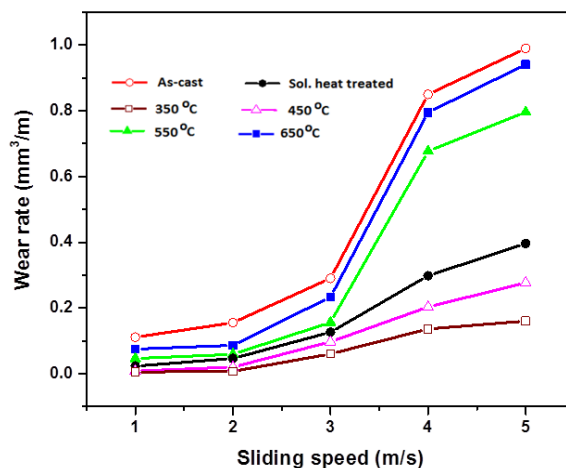


Fig.7. Effect of sliding speed on wear rate of the as-cast and heat treated Cu-Al-Fe-Ni alloy

The surface roughness of heat treated specimens at an applied load of 15 N and a sliding velocity of 3.0 m/s is presented in Fig. 10. It can be seen that the surface roughness increases with rising aging temperature. This means that increasing aging temperature increases the deformation zones by stimulating the plastic flow of the material during abrasive action of grit [16]. The presented results are in agreement with the results of the other sections.

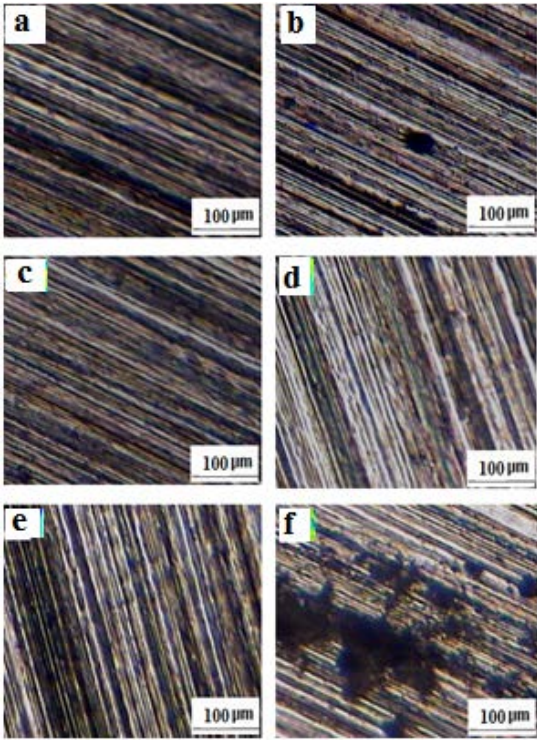


Fig.8. SEM micrographs of worn surfaces of heat treated Cu-Al-Fe-Ni alloy [(a) as-cast, (b) Sol. heat treated at 960 °C, (c) 350 °C, (d) 450 °C, (e) 550 °C and (f) 650 °C]

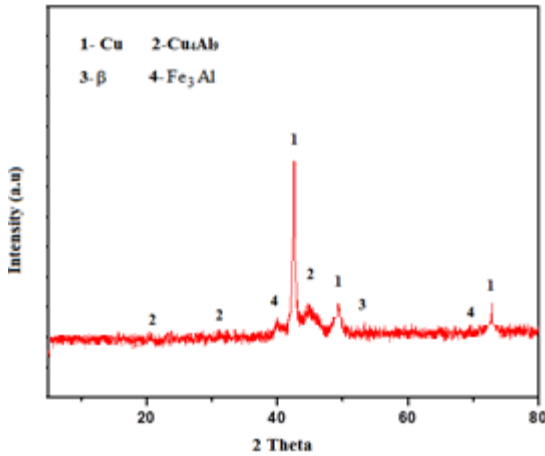


Fig.9. XRD of the abraded powder for specimen aged 350 °C

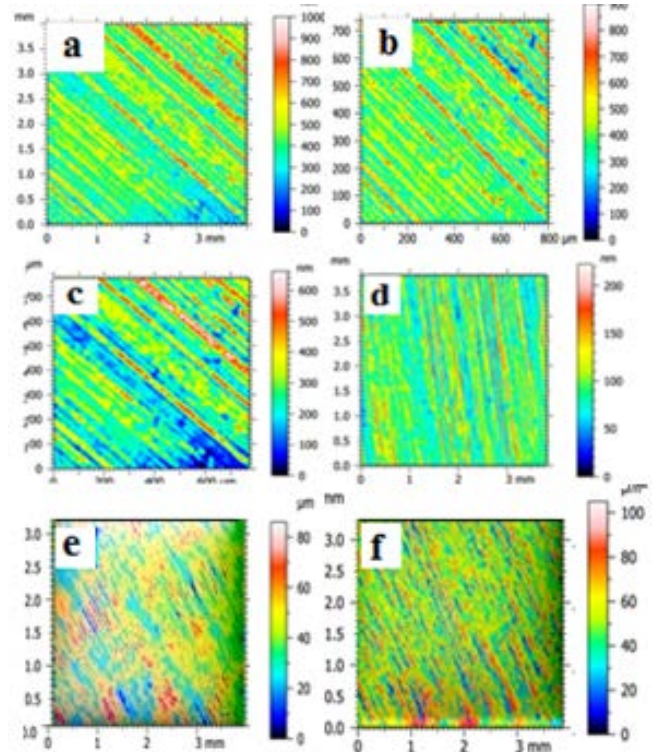


Fig.10. The 3-dimensional surface profiles of heat treated Cu-Al-Fe-Ni alloy at an applied load of 15 N and a sliding speed of 3.0 m/s. [(a) as-cast, (b) Sol. heat treated at 960 °C, (c) 350 °C, (d) 450 °C, (e) 550 °C and (f) 650 °C]

### 3.3.4. Effect of heat treatment on temperature rise

The temperature rise of the as-cast and heat treated specimens at an applied load of 15 N and a sliding velocity of 3.0 m/s is shown in Fig. 11. It is obvious that at the initial stage of the wear tests the temperature increases rapidly with increasing the time of wear for all specimens to about 100 Sec. This behaviour is attributed to the high hardness of the oxide layer on the surfaces of samples. After certain time the temperature rise tends to reach a steady value due to the abraded particles which work as a lubricant. However, sample aged at 350 °C exhibits the lowest temperature rise comparing to the other samples, which implies the lowest energy and dissipation. Therefore it has the lowest coefficient of friction. On the other hand, increasing the aging temperature as shown in Fig.11 leads to increasing temperature rise. This behaviour is due to transforming large amount of  $\beta$ -phase into precipitates of  $\alpha$ -particles with large size which are softer comparing to  $\beta$ -phase. This means that increasing aging temperature leads to increasing the energy and

dissipation of Cu-Al-Fe-Ni alloy and consequently increasing the coefficient of friction.

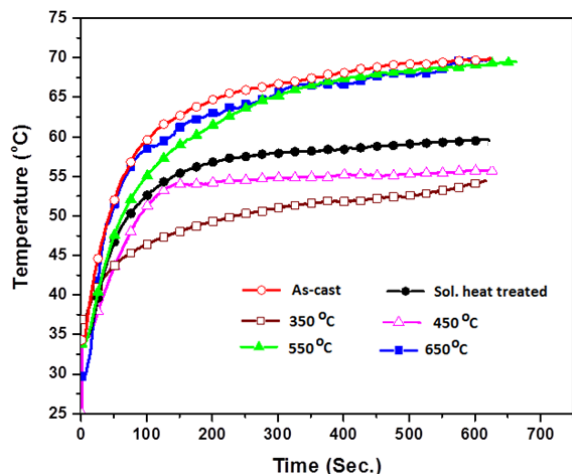


Fig.11. The temperature rise of as-cast and heat treated Cu-Al-Fe-Ni alloy at an applied load of 15 N and a sliding speed of 3.0 m/s

#### 4. Conclusions

In this paper, the effect of heat treatment on microstructure and dry sliding wear behaviour of Cu-Al-Fe-Ni alloy was investigated. The following conclusions were reached:

- 1- Quenching of Cu-Al-Fe-Ni causes all  $\beta$  phase transformed into  $\beta'$  phase. However aging heat treatment causes the transformation of  $\beta'$  martensite into  $\alpha$  and fine  $\kappa$  phases.
- 2- Hardness of Cu-Al-Fe-Ni can be significantly improved by solution heat treated at 960°C for 5h followed by aging at 350°C for 5h.
- 3- Increasing the aging temperature causes the grains and the eutectoid precipitates to coarsen.
- 4- Increasing the applied load and sliding speed increased the wear rate. However, the aged sample at 350°C offered the highest wear resistance.
- 5- The worn surfaces revealed that the predominant wear mechanism was abrasive wear for as-cast and heat treated Cu-Al-Fe-Ni alloy.

#### 5. References

[1] Sadawy, M. M. and Ghanem, M., "Grain refinement of bronze alloy by equal-channel angular pressing (ECAP) and its effect on corrosion behaviour", *Defence Technology* 12, 2016, pp. 316–323

- [2] Zohdy, K.M., Sadawy, M.M. and Ghanem, M., "Corrosion behavior of leaded-bronze alloys in sea water", *Materials Chemistry and Physics* 147, 2014, 878–883
- [3] Abd-Elmonem Metwally, M., Sadawy, M.M., Ghanem, M. and EL-Batanony, I.G., "Effect of SiC content on the corrosion behavior of nanosized SiC(p)/Cu composites" *The Egyptian International Journal of Engineering Sciences and Technology*, 26, 2018, pp. 22–28
- [4] Ragaba, Kh.A., Abdel-Karim, R., Farag, S., El-Raghy, S.M. and Ahmed, H.A., "Influence of SiC, SiO<sub>2</sub> and graphite on corrosive wear of bronze composites subjected to acid rain", *Tribology International*, 43, 2010, pp. 594–601
- [5] J.M. Gomez de Salazar, A. Soria, M.I. Barrena Corrosion behaviour of Cu-based shape memory alloys, diffusion bonded, *Journal of Alloys and Compounds* 387 (2005) pp.109–114
- [6] M. Colic, R. Rudolf, D. Stamenkovic, I. Anzel, D. Vucevic, M. Jenkoc, V. Lasic, G. Lojen, Relationship between microstructure, cytotoxicity and corrosion properties of a Cu–Al–Ni shape memory alloy, *Acta Biomaterialia* 6 (2010), pp. 308–317
- [7] S. Montecinos, S.N. Simison, Influence of the microstructure on the corrosion behaviour of a shape memory Cu–Al–Be alloy in a marine environment, *Applied Surface Science* 257 (2011) pp.2737–2744
- [8] Safaa N. Saud, E. Hamzah, T. Abubakar, H.R. Bakhsheshi-Rad, S. Farahany, A. Abdolahi, M.M. Taheri, Influence of Silver nanoparticles addition on the phase transformation, mechanical properties and corrosion behaviour of Cu–Al–Ni shape memory alloys, *Journal of Alloys and Compounds* 612 (2014), pp. 471–478
- [9] Hosny, A. M., "Effect of heat treatment on corrosion and wear of aluminum bronze alloy reinforced with austenitic stainless steel particles" Thesis, Degree M.Sc, Faculty of Engineering, Department of Mining and Metallurgical Engineering, Al-Azhar University, 2017, pp. 1–96.
- [10] Z. Wu, Y. F. Cheng, L. Liu, W. Lv, W. Hu, Effect of heat treatment on microstructure evolution and erosion–corrosion behavior of a nickel–aluminum bronze alloy in chloride solution, *Corrosion Science* 98 (2015), pp. 260–270
- [11] Jain, P. and Nigam, P. K., "Influence of Heat Treatment on Microstructure and Hardness of Nickel Aluminium Bronze (Cu-10Al-5Ni-5Fe)", *IOSR Journal of Mechanical and Civil Engineering*, 6, 4, 2013, pp.16-21
- [12] Sabbaghzadeh, B., Parvizi, R., Davoodi, A. and Moayed, M. H., "Corrosion evaluation of multi-pass welded nickel–aluminum bronze alloy in 3.5% sodium chloride solution: A restorative application of gas tungsten arc welding process", *Materials and Design*, 58, 2014, pp. 346–356
- [13] Sláma, P., Dlouhý, J. and Kövér, M.I. Influence of heat treatment on the microstructure and mechanical properties of aluminum bronze" *Materials and technology*, 48, 2, 2014, pp. 599–604
- [14] Pisarek, B. P., "Effect of annealing time for quenching (Cu-Al7-Fe5-Ni5-W2-Si2) bronze on the microstructure and mechanical properties" *Archives of Foundry Engineering*, 12, 2, 2012, pp. 187-2
- [15] Chen, R.P., Liang, Z.Q., Zhang, W.W., Zhang, D.T., Luo, Z.Q. and Li, Y.Y. "Effect of heat treatment on microstructure and properties of hot-extruded nickel–aluminum bronze" *Trans Nonferrous Met Soc China*, 17, 6, 2007, pp.1254–1258
- [16] Agunsoye, J.O. and Ayen, A.A., "Effect of Heat Treatment on the Abrasive Wear Behavior of High Chromium Iron under Dry Sliding Condition" *Tribology in Industry*, 34, 2, 2012, pp. 82-91

- [17] Babic, M. Mitrovic, S. and Jeremic, B., "The influence of heat treatment on the sliding wear behavior of a ZA-27 alloy", *Tribology International*, 43 ,2010, ,pp. 16–21
- [18] Mao-liang, H., Qu-dong, W., Cheng, L. and Wen-jiang, D. "Dry sliding wear behavior of cast Mg-Y-5Gd-2Zn magnesium alloy" *Trans. Nonferrous Met. S<sup>o</sup>C. China* 22, 2012, pp. 1918-1923
- [19] Kaushik, N.Ch. and Rao, R.N., "Effect of applied load and grit size on wear coefficients of Al 6082–SiC–Gr hybrid composites under two body abrasion" *Tribology International*, 103,2016, pp. 298–308